The electromagnetic response of a disk beneath an exponentially varying conductive overburden

P. F. Siew[*]   S. Yooyuanyong[†]

Abstract

Integral equations that give the electromagnetic response of a thin disk situated beneath an inhomogeneous conductive overburden are

[*]School of Maths and Stats, Curtin University of Tech, GPO Box U1987, Perth, Western Australia 6001, AUSTRALIA.

[†]Dept of Maths, Faculty of Science, Silpakorn University, Nakorn-pathom 74000, THAILAND.

derived, and expressions for the electric fields in the overburden and on the disk are given. The equations obtained can be used to estimate unknown parameters such as, the conductance and the depth of burial of the disk, as well as the thickness of the overburden. The estimation of the above parameters is important in the identification of subsurface structures. An inversion procedure is outlined whereby the optimal values for these parameters is obtained by an iterative technique.

Contents

1   Introduction

Many techniques have been used in exploration geophysics to obtain information about the structure of the ground from surface measurements. Among these, the analysis of electromagnetic field data is of great interest because it is far less expensive than most other investigation methods. The interpretation of electromagnetic data is frequently done assuming the subsurface to consist of horizontal layers, where each layer has a constant electrical conductivity. For instance, Ryu *et al* [12] obtained integral expressions for the electromagnetic field responses due to a horizontal loop above the surface of a multi-layered half-space. A more realistic model may involve a half-space with a continuously varying conductivity profile. The linearized inverse theory of Backus and Gilbert [2, 3] has been used by several authors to estimate the continuous resistivity profile of the earth (see for example, Oldenburg [10] and Parker [11]. Lee and Ignetik [9] considered the forward problem involving a half-space with an exponentially varying conductivity profile. Buselli and Williamson [5] used airborne electromagnetic data to invert for the salinity profiles using layered models. Rough correlation for the model parameters were obtained through electric conductivity logs. However, a more useful model may be nearer the type of profiles used by Kim and Lee [8] who used the direct current method to consider models where each layer has an exponentially varying conductivity. Siew and Yooyuanyong [13] developed an algorithm to solve the inverse problem for finding the conductance and the depth of a thin disk embedded within a half-space with an exponentially varying conductivity, using electromagnetic measurements

on the earth's surface.

As remarked in [9], the conductivity profiles in some areas, especially in coastal plains or sedimentary basins, exhibit a monotonic decreasing characteristic. This variation may sometimes be reasonably approximated by an exponentially decreasing conductivity profile. In the present paper, we consider a thin disk, embedded in a resistive host medium for which the conductivity is assumed to be zero. The disk is located beneath a conductive overburden, with an exponentially varying conductivity profile. The objective of this paper is to present a technique whereby the electromagnetic observations obtained from a vertical magnetic dipole above the ground surface is inverted to determine the thickness of the overburden, the conductance, and the depth of the disk.

2   Derivation of Electromagnetic Field

Consider a primary alternating source current carried by a coil of radius a, at $z = -h$ above the surface of the earth ($z = 0$). The source current density, with frequency ω, is given by $J_{s\theta} = I(\omega)a\delta(r - a)\delta(z + h)\exp(i\omega t)/r$, where $I(\omega)$ is the current in the coil, and cylindrical coordinates (r, θ, z), with $z > 0$ taken vertically downwards and origin below the centre of the coil, are used. An overburden, with a conductivity given by $\sigma_p(z) = \sigma_1 e^{-bz}$, where b and σ_1 are positive constants, occupies the region $0 \le z \le d_1$ (see Figure 1). A horizontally orientated thin circular body, with a constant conductivity σ_s,
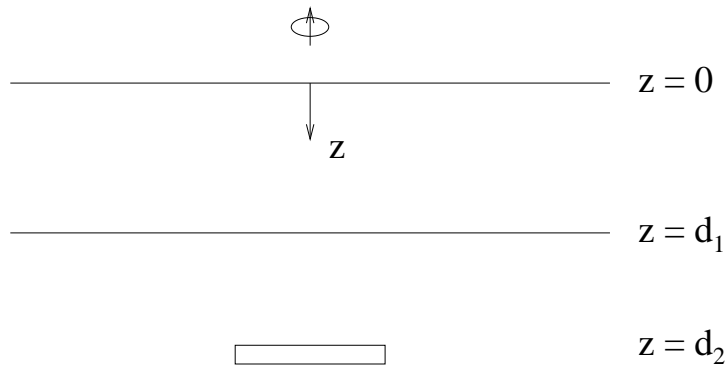
FIGURE 1: physical layout showing the z axis downwards, the source above $z = 0$, and the body below $z = d_2$.

is located below the origin in a resistive host medium. The thickness d, of the body is assumed to be small compared to its radius c ($d \ll c$), and the centre of the body is located beneath the origin at $z = d_2$, $(d_2 > d_1)$.

By symmetry, there is only an azimuthal component of the electric field, E. From now on, a time variation $\exp(i\omega t)$ is assumed throughout, and the governing equations are

$$i\omega\mu_0 H_r = \frac{\partial E}{\partial z}, \tag{1}$$

$$i\omega\mu_0 H_z = -\frac{1}{r}\frac{\partial(rE)}{\partial r}, \tag{2}$$

and

$$\frac{\partial H_r}{\partial z} - \frac{\partial H_z}{\partial r} = \sigma(z)E + J_{s\theta} \,, \tag{3}$$

where H_r and H_z are the radial and vertical components respectively of the magnetic field. Assuming the medium is non-magnetic, the magnetic permeability of free space, μ_0, is used throughout. Further, the quasi-stationary approximation has been made. As explained in Grant and West [7, Ch. 16] this approximation can be made for most earth structures, where the electromagnetic phenomenon involves induction only, without propagation effects. Effectively, this means that the velocity scale associated with the problem under study is small compared to the speed of light and hence the displacement current term in Maxwell's equations may be neglected. In equation (3) above, $\sigma(z)$ is the conductivity, which is zero in air and in the resistive medium, but is given by $\sigma_p(z)$ and σ_s respectively in the overburden and in the circular disk. Eliminating H_r and H_z from the above equations leads to

$$\frac{\partial^2 E}{\partial z^2} + \frac{\partial^2 E}{\partial r^2} + \frac{1}{r}\frac{\partial E}{\partial r} - \frac{E}{r^2} - k^2 E = i\omega\mu_0 J_{s\theta} \,, \tag{4}$$

where $k^2 = i\omega\mu_0\sigma(z)$. Taking the Hankel transform with respect to r, defined by

$$\widetilde{E}(\lambda, z, \omega) = \int_0^\infty r J_1(\lambda r) E(r, z, \omega) \, dr \,,$$

equation (4) becomes

$$\frac{\partial^2 \widetilde{E}}{\partial z^2} - (\lambda^2 + k^2)\widetilde{E} = i\omega\mu_0 I(\omega) a J_1(\lambda a)\delta(z + h) \,. \tag{5}$$

In air, $k = 0$ and the electric field is given by

$$\widetilde{E}_{\text{air}}(\lambda, z, \omega) = -\frac{i\omega\mu_0 aI(\omega)J_1(\lambda a)e^{-\lambda|z+h|}}{2\lambda} + C_1 e^{\lambda z}, \quad z \leq 0, \qquad (6)$$

which remains bounded as $z \to -\infty$, and C_1 is a constant to be determined.

The transformed electric field in the overburden, $\widetilde{E}_{\text{ove}}$, is obtained from the homogeneous form of (5) with $\sigma(z)$ replaced by $\sigma_p(z)$. Following Lee & Ignetik [9], the coordinate transformation $\zeta = \exp(-bz/2)$ is used to convert the differential equation to

$$\left[\zeta^2 \frac{d^2}{d\zeta^2} + \zeta\frac{d}{d\zeta} - (\alpha^2\zeta^2 + \nu^2)\right]\widetilde{E}_{\text{ove}} = 0, \quad 0 \leq z \leq d_1, \qquad (7)$$

where $\alpha^2 = 4i\mu_0\sigma_1\omega/b^2$ and $\nu^2 = 4\lambda^2/b^2$. The solution to (7) is

$$\widetilde{E}_{\text{ove}} = BI_\nu(\alpha\zeta) + CK_\nu(\alpha\zeta), \quad 1 \leq \zeta \leq \zeta_1 \qquad (8)$$

where B and C are arbitrary constants, I_ν and K_ν are the modified Bessel functions of the first and the second kind of order ν, and $\zeta_1 = \exp(-bd_1/2)$.

In the resistive medium beneath the overburden ($z \geq d_1$), we denote the electric field by $E_{\text{host}} = E^p + E^s$, where E^p is the field in the absence of the circular disk, and E^s is the electric field due to the presence of the disk. Since the conductivity is now zero, except in the circular disk, the electric fields satisfy the equations

$$\frac{\partial^2 E^p}{\partial z^2} + \frac{\partial^2 E^p}{\partial r^2} + \frac{1}{r}\frac{\partial E^p}{\partial r} - \frac{E^p}{r^2} = 0 \qquad (9)$$

and

$$\frac{\partial^2 E^s}{\partial z^2} + \frac{\partial^2 E^s}{\partial r^2} + \frac{1}{r}\frac{\partial E^s}{\partial r} - \frac{E^s}{r^2} - k_s^2 E = 0 \,. \tag{10}$$

where, for convenience, we let $k_s^2 = i\omega\mu_0\sigma_s$ on the disk and is zero elsewhere. Taking Hankel transforms as before, the two equations above become, respectively,

$$\frac{\partial^2 \widetilde{E}^p}{\partial z^2} - \lambda^2 \widetilde{E}^p = 0 \,, \tag{11}$$

and

$$\frac{\partial^2 \widetilde{E}^s}{\partial z^2} - \lambda^2 \widetilde{E}^s = i\omega\mu_0 \int_0^c \sigma_s E_d s J_1(\lambda s)\, ds \,, \tag{12}$$

where E_d is the electric field on the disk. $\sigma_s E_d$ may be viewed as an equivalent current distribution on the disk. The bounded solution for equation (11) is

$$\widetilde{E}^p = A_1 e^{-\lambda z}, \quad z \geq d_1 \,, \tag{13}$$

where A_1 is an arbitrary constant. The transformed electric field due to the presence of the disk, $\widetilde{E}^s$, is obtained from (12) by using the method of variation of parameters, and the solution may be written as

$$\widetilde{E}^s = A_2 e^{-\lambda z} - \frac{1}{2\lambda}\int_z^\infty e^{-\lambda(x-z)} f(x)\, dx - \frac{1}{2\lambda}\int_{d_1}^z e^{\lambda(x-z)} f(x)\, dx \,, \tag{14}$$

where $f(z) = i\omega\mu_0 \int_0^c \sigma_s E_d s J_1(\lambda s)\, ds$ and A_2 is a constant. This solution is bounded as $z \to \infty$ and hence, combining with (13), the solution below the overburden is given by

$$\widetilde{E}_{\text{host}} = -\frac{i\omega\mu_0}{2\lambda}\int_{d_1}^\infty \int_0^c \sigma_s s E_d J_1(\lambda s)\, ds\, G(z; x)\, dx + R e^{-\lambda z} \,, \tag{15}$$

where R is an arbitrary constant to be determined, and $G(z;x) = e^{-\lambda|z-x|}$ is the Green's function. $\sigma_s E_d$ is zero except over the thickness $d_2 - d/2 < z < d_2 + d/2$ on the disk. For a thin disk, a Taylor series expansion now yields

$$\widetilde{E}_{\text{host}}(\lambda, z, \omega) = -\frac{i\omega\mu_0}{2\lambda} \int_0^c \sigma_s s E_d(s, d_2, \omega) J_1(\lambda s) ds\, G(z; d_2) d + R e^{-\lambda z} . \quad (16)$$

Let the conductance $S = d\sigma_s$, then (16) becomes

$$\widetilde{E}_{\text{host}}(\lambda, z, \omega) = -\frac{i\omega\mu_0}{2\lambda} \int_0^c S s E_d(s, d_2, \omega) J_1(\lambda s) ds\, G(z; d_2) + R e^{-\lambda z} , \quad z \geq d_1 . \quad (17)$$

The arbitrary constants are now solved by imposing the continuity of E and $\partial E/\partial z$ at each of the interfaces giving

$$B = -\frac{2\nu}{\alpha\beta D} \left[\alpha\psi K_{\nu-1}(\alpha) + \beta\gamma K_{\nu+1}(\beta)\right] ,$$

$$C = -\frac{2\nu}{\alpha\beta D} \left[\alpha\psi I_{\nu-1}(\alpha) + \beta\gamma I_{\nu+1}(\beta)\right] ,$$

$$C_1 = \gamma - \frac{2\nu}{\alpha\beta D} \left[\psi + \beta\gamma \left\{I_\nu(\alpha)K_{\nu+1}(\beta) + I_{\nu+1}(\beta)K_\nu(\alpha)\right\}\right] ,$$

and

$$R = \psi e^{\lambda d_1} - \frac{2\nu e^{\lambda d_1}}{\alpha\beta D} \left[\gamma + \alpha\psi \left\{K_{\nu-1}(\alpha)I_\nu(\beta) + I_{\nu-1}(\alpha)K_\nu(\beta)\right\}\right] ,$$

where $\beta = \alpha\zeta_1$,

$$\psi = \frac{i\omega\mu_0 e^{-\lambda(d_2-d_1)}}{2\lambda} \int_0^c s J_1(\lambda s) S E_d \, ds ,$$

$$\gamma = \frac{i\omega\mu_0 a I(\omega)J_1(\lambda a)e^{-\lambda h}}{2\lambda},$$
$$\text{and} \quad D = K_{\nu+1}(\beta)I_{\nu-1}(\alpha) - K_{\nu-1}(\alpha)I_{\nu+1}(\beta).$$

Thus, the electric field in the various regions are

$$\widetilde{E}_{\text{air}}(\lambda, z, \omega) = -\frac{i\omega\mu_0 a I(\omega)J_1(\lambda a)e^{-\lambda|z+h|}}{2\lambda} + \gamma e^{\lambda z}$$
$$- \frac{2\nu e^{\lambda z}}{\alpha\beta D}\{\psi + \beta\gamma[I_\nu(\alpha)K_{\nu+1}(\beta) + I_{\nu+1}(\beta)K_\nu(\alpha)]\}, (18)$$

$$\widetilde{E}_{\text{ove}}(\lambda, z, \omega) = -\frac{2\nu}{\alpha\beta D}\{[\alpha\psi K_{\nu-1}(\alpha) + \beta\gamma K_{\nu+1}(\beta)]I_\nu(\alpha\zeta)$$
$$+ [\alpha\psi I_{\nu-1}(\alpha) + \beta\gamma I_{\nu+1}(\beta)]K_\nu(\alpha\zeta)\}, \qquad (19)$$

and

$$\widetilde{E}_{\text{host}}(\lambda, z, \omega) = -\frac{i\omega\mu_0}{2\lambda}\int_0^c sSE_dJ_1(\lambda s)ds e^{-\lambda|z-d_2|}$$
$$+ e^{-\lambda(z-d_1)}\left\{\psi - \frac{2\nu}{\alpha\beta D}[\gamma + \alpha\psi(K_{\nu-1}(\alpha)I_\nu(\beta) + I_{\nu-1}(\alpha)K_\nu(\beta))]\right\}(20)$$

Another expression that we require later is the electric field on the surface of the earth which is

$$\widetilde{E}_{\text{ove}}(\lambda, 0, \omega) = -\frac{2\nu}{\alpha\beta D}\{\psi + \beta\gamma[K_{\nu+1}(\beta)I_\nu(\alpha) + I_{\nu+1}(\beta)K_\nu(\alpha)]\}. \qquad (21)$$

If the disk is absent ($S = 0$) and if we allow d_1 to tend to infinity, we recover from (18) the result obtained in [9] for the response of a halfspace with an exponentially varying conductivity profile. On the other hand, if the overburden is absent, we put $d_1 = 0$, $\beta = \alpha$, and hence, taking the inverse Hankel transforms of equation (20), we recover the integral equation for the response due to a disk in free space, which may be derived from the result given in Appendix A in [14].

The electric fields due to an oscillating magnetic dipole can readily be obtained from equations (18) to (21) (see [7] for example). Thus, for a dipole source of moment $M = \pi a^2 I(\omega)$ on the surface of the ground ($h = 0$), we have $\gamma = i\omega\mu_0 M/(4\pi)$, and hence, the field quantities in the physical domain are given by

$$
\begin{aligned}
E_{\text{air}}(r, z, \omega) \ = \ & -\frac{4}{\alpha b} \int_0^\infty \frac{\lambda^2 e^{\lambda z} J_1(\lambda r)}{\beta D} \times \\
& \{\psi + \beta\gamma[I_\nu(\alpha)K_{\nu+1}(\beta) + I_{\nu+1}(\beta)K_\nu(\alpha)]\} \, d\lambda, \quad (22)
\end{aligned}
$$

$$
\begin{aligned}
E_{\text{ove}}(r, z, \omega) \ = \ & -\frac{4}{\alpha b} \int_0^\infty \frac{\lambda^2 J_1(\lambda r)}{\beta D} \{[\alpha\psi K_{\nu-1}(\alpha) + \beta\gamma K_{\nu+1}(\beta)]I_\nu(\alpha\zeta) \\
& + [\alpha\psi I_{\nu-1}(\alpha) + \beta\gamma I_{\nu+1}(\beta)]K_\nu(\alpha\zeta)\} \, d\lambda, \quad (23)
\end{aligned}
$$

and

$$
E_{\text{host}} = -\frac{i\omega\mu_0}{2} \int_0^c sSE_d \, ds \int_0^\infty e^{-\lambda|z-d_2|} J_1(\lambda r) J_1(\lambda s) d\lambda
$$

$$+ \int_0^\infty \lambda e^{-\lambda(z-d_1)} J_1(\lambda r) \times$$

$$\left\{ \psi - \frac{4\lambda}{\beta \alpha b D} [\gamma + \alpha\psi(K_{\nu-1}(\alpha)I_\nu(\beta) + I_{\nu-1}(\alpha)K_\nu(\beta))] \right\} d\lambda. \quad (24)$$

On the surface of the ground we have

$$E_{\text{ove}}(r, 0, \omega) = -\frac{4}{ab} \int_0^\infty \frac{\lambda^2 J_1(\lambda r)}{\beta D} \left\{ \psi + \beta\gamma[K_{\nu+1}(\beta)I_\nu(\alpha) + I_{\nu+1}(\beta)K_\nu(\alpha)] \right\} d\lambda. \quad (25)$$

In general, the magnitude of the measured electric field tends to be small, compared to unity, and so it is expedient to scale it by using $E^* = -EL^2/\gamma$, where L is a length scale. (In the subsequent numerical computation L is taken to be d_2.) If Ω is a typical frequency, the non-dimensional quantities are given by $r^* = r/L$, $s^* = s/L$, $c^* = c/L$, $\lambda^* = \lambda L$, $S^* = \Omega\mu_0 LS$, $\omega^* = \omega/\Omega$, $b^* = bL$ and

$$\psi^* = \frac{\psi}{\gamma} = -\frac{i\omega^* e^{-\lambda^*(d_2^*-d_1^*)}}{2\lambda^*} \int_0^{c^*} s^* S^* E_d^* J_1(\lambda^* s^*) ds^*.$$

Dropping asterisks from now on, the non-dimensional form of the electric fields that we will require are

$$E_{\text{ove}}(r, z, \omega) = -\frac{2i\omega}{b} \int_0^c sSE_d \, ds \int_0^\infty \frac{\lambda J_1(\lambda s) J_1(\lambda r) e^{-\lambda(d_2-d_1)}}{\beta D} \times$$

$$[K_{\nu-1}(\alpha)I_\nu(\alpha\zeta) + I_{\nu-1}(\alpha)K_\nu(\alpha\zeta)] d\lambda$$

$$+ \frac{4}{\alpha b} \int_0^\infty \frac{\lambda^2 J_1(\lambda r)}{D}[K_{\nu+1}(\beta)I_\nu(\alpha\zeta) + I_{\nu+1}(\beta)K_\nu(\alpha\zeta)]d\lambda\,,$$
$$0 < z < d_1\,, \tag{26}$$

$$\begin{aligned}
E_{\text{host}}(r,z,\omega) &= -\frac{i\omega}{2}\int_0^c sSE_d\,ds\int_0^\infty e^{-\lambda|z-d_2|}J_1(\lambda r)J_1(\lambda s)d\lambda \\
&\quad + \frac{i\omega}{2}\int_0^c sSE_d\,ds\int_0^\infty e^{-\lambda(z+d_2-2d_1)}J_1(\lambda r)J_1(\lambda s)\times \\
&\quad \left\{1 - \frac{4\lambda}{\beta bD}[K_{\nu-1}(\alpha)I_\nu(\beta) + I_{\nu-1}(\alpha)K_\nu(\beta)]\right\}d\lambda \\
&\quad + \frac{4}{\alpha b}\int_0^\infty \frac{\lambda^2 e^{-\lambda(z-d_1)}}{\beta D}J_1(\lambda r)d\lambda\,, \quad z > d_2, \tag{27}
\end{aligned}$$

and

$$\begin{aligned}
E_{\text{ove}}(r,0,\omega) &= -\frac{2i\omega}{\alpha b}\int_0^c sSE_d\,ds\int_0^\infty \frac{\lambda e^{-\lambda(d_2-d_1)}J_1(\lambda s)J_1(\lambda r)}{\beta D}d\lambda \\
&\quad + \frac{4}{\alpha b}\int_0^\infty \frac{\lambda^2 J_1(\lambda r)}{D}[K_{\nu+1}(\beta)I_\nu(\alpha) + I_{\nu+1}(\beta)K_\nu(\alpha)]d\lambda\,. \tag{28}
\end{aligned}$$

We note that $I_{\nu-1}(\alpha)$ never vanishes since the zeros of $J_{\nu-1}(w)$ in the complex w-plane are all real, see [1, pp.372 & 375]. Also, we note that $\beta < \alpha = \sqrt{4i\omega\mu_0\sigma_1}/|b| \ll 1$ and expanding about β we have

$$I_{\nu-1}(\alpha) = I_{\nu-1}(\beta) + (\alpha - \beta)\left[I_\nu(\beta) + \frac{(\nu-1)}{\beta}I_{\nu-1}(\beta)\right] + \mathcal{O}\left[(\alpha - \beta)^2\right]\,,$$

and

$$K_{\nu-1}(\alpha) = K_{\nu-1}(\beta) + (\alpha - \beta) \left[-K_\nu(\beta) + \frac{(\nu - 1)}{\beta} K_{\nu-1}(\beta) \right] + \mathcal{O}\left[(\alpha - \beta)^2 \right] .$$

Hence

$$
\begin{aligned}
D &= K_{\nu+1}(\beta)I_{\nu-1}(\alpha) - K_{\nu-1}(\alpha)I_{\nu+1}(\beta) \\
&\sim \frac{2\nu}{\beta^2} + \frac{(\alpha - \beta)}{\beta} \left[1 + \frac{2\nu(\nu - 1)}{\beta^2} \right] + \mathcal{O}\left[(\alpha - \beta)^2 \right] ,
\end{aligned}
$$

which never vanishes. Hence, the integrals in (26), (27) and (28) are all well defined. The electric field on the disk is determined from (27) by taking $z = d_2$, thus we have

$$
\begin{aligned}
E_d &= -\frac{i\omega}{2} \int_0^c sH(s,\omega)ds \int_0^\infty J_1(\lambda r)J_1(\lambda s)d\lambda \\
&+ \frac{i\omega}{2} \int_0^c sH(s,\omega)ds \int_0^\infty e^{-2\lambda(d_2-d_1)}J_1(\lambda r)J_1(\lambda s) \times \\
&\quad \left\{ 1 - \frac{4\lambda}{\alpha b D} \left[K_{\nu-1}(\alpha)I_\nu(\beta) + I_{\nu-1}(\alpha)K_\nu(\beta) \right] \right\} d\lambda \\
&+ \frac{4}{\alpha b} \int_0^\infty \frac{\lambda^2 e^{-\lambda(d_2-d_1)}}{\beta D} J_1(\lambda r)d\lambda ,
\end{aligned}
\tag{29}
$$

where $H(s,\omega) = SE_d$ is the integrated current density on the disk. If the true depths d_1 and d_2 are known then equation (28) can be used to estimate the function $H(s,\omega)$, assuming the field on the surface is known. Equation (29)

can be then used to find the true value of the conductance S. However, in practice, this may not be the order the two equations are used since, d_1, d_2 and S are unknown, and usually, an iterative process needs to be employed to successively find improved estimates starting with initial guesses. When the estimates for d_1, d_2 and S are close to their true values, we expect the electric field to be close to its true value also.

The integrals in (26)–(29) can be all put in the form $\int_0^\infty \lambda J_1(\lambda r) f(\lambda) d\lambda$, where $f(\lambda)$ is a complex function of λ. Integrals of this form can be evaluated using an algorithm, due to Chave [4], which is an efficient direct integration scheme giving numerical results of high accuracy. In his paper, Chave considered examples where $f(\lambda)$ is either exponentially decreasing, constant, slowly increasing or oscillatory. In the current problem the complex function typically involves the modified Bessel functions of the first and second kind, of fractional order ν or $\nu - 1$, and the arguments, in each case, are pure imaginary. The values of the modified Bessel functions are computed using standard NAG routines.

3   An Iterative Procedure

Suppose we have a complex data array $\left\{ \boldsymbol{E}^{(d)} \right\}$, which is obtained from measurements of the electric field on the surface of the earth. The most popular method used to obtain such an array is to measure the electric field at a fixed transmitter/receiver separation spacing r at various frequencies ω_i, so

that the ith entry in the data array is $E_i^{(d)} = E(r, 0, \omega_i)$, $i = 1, 2, \ldots,$ N. Alternatively, the data array may be collected by use of a fixed source method whereby readings may be taken at various transmitter/receiver spacings r_i at a fixed frequency ω. In this case the ith entry in the data array is $E_i^{(d)} = E(r_i, 0, \omega)$. The derivation given here applies no matter which method is used to generate the data array. If at the jth step we have estimates of the depths $d_1^{(j)}$, $d_2^{(j)}$ and the conductance $S^{(j)}$, these values are used in (29) to obtain an estimate for $H(s, \omega)$. In the numerical scheme, the disk is divided into N rings of thickness $\Delta = c/N$. If the radius of the ith ring is s_i, then (29) is replaced by the linear system

$$[U_{ji} + \delta_{ji}] H_i = Q_j, \tag{30}$$

where $H_i = H(s_i, \omega)$, δ_{ji} is the Kronecker delta,

$$Q_j = \frac{4S}{\alpha b \beta} \int_0^\infty \frac{\lambda^2 e^{-\lambda(d_2 - d_1)} J_1(\lambda s_j)}{D} \, d\lambda$$

and

$$
\begin{aligned}
U_{ji} &= \frac{i\omega \Delta S s_i}{2} \int_0^\infty \left[1 - e^{-2\lambda(d_2 - d_1)} \right] J_1(\lambda s_i) J_1(\lambda s_j) d\lambda \\
&= \frac{2 i \omega \Delta S s_i}{b \alpha} \int_0^\infty \lambda e^{-2\lambda(d_2 - d_1)} J_1(\lambda s_i) J_2(\lambda s_j) \times \\
&\qquad \frac{K_{\nu-1}(\alpha) I_\nu(\beta) + K_\nu(\beta) I_{\nu-1}(\alpha)}{D} \, d\lambda.
\end{aligned}
$$

Each of the above integrals is evaluated using Chave's algorithm. The solution of (30) now gives the distribution of the integrated current density on the disk.

Once $H(s_i, \omega)$, $i = 1, 2, \ldots, N$ are known, (28) is used to obtain the calculated electric field array $\{\mathbf{E}^{(j)}\}$. From these, we obtain the difference vector $\mathbf{E}^{(j)} - \mathbf{E}^{(d)}$. The magnitude of this difference vector is a function of the difference between the observed and the calculated electric field over the interval at which readings are taken. It is therefore necessary to obtain expressions which link the change in the electric field to the changes in the values of d_1, d_2 and S. The expression linking a small change in the electric field due to a change in the conductivity at depth z is given by the Fréchet kernel derived by Fullagar and Oldenburg [6] and is written in terms of the transform space as

$$\delta \widetilde{E}(\lambda, 0, \omega) = -\frac{i\omega\mu}{2\lambda \widetilde{E}(\lambda, 0, \omega)} \int_0^\infty \widetilde{E}^2(\lambda, z, \omega)\delta\sigma(z)dz \,.$$

Assuming that d_1 and d_2 are known, the change in conductivity is linked to the error in estimating S. In effect, if the conductivity changes by $\delta\sigma$ over the small thickness d, of the disk only, we write

$$\delta \widetilde{E}(\lambda, 0, \omega) = -\frac{i\omega\mu_0(\delta S)\widetilde{E}^2(\lambda, d_2, \omega)}{2\lambda \widetilde{E}(\lambda, 0, \omega)} \,, \tag{31}$$

where $\delta S = d\, \delta\sigma$. The inversion of (31) gives the change, δE, due to a change in the conductance. Since $\mathbf{E}^{(d)}$ is a constant vector, the change in $\mathbf{E}^{(j)}$ at the jth step is interpreted as the change in the difference vector $\mathbf{E}^{(j)} - \mathbf{E}^{(d)}$ also. The vector $\delta\mathbf{E}^{(j)}/\delta S$ gives an average rate of change of the difference vector with respect to a change in the conductance. The norm of this rate of change

vector then gives an estimate of the absolute value of the rate of change of the difference norm $\Delta E^{(j)} = \|\mathbf{E}^{(j)} - \mathbf{E}^{(d)}\|$ with respect to S over the range of data values used. The expressions linking a small change in the electric field to the depths d_1 and d_2 are found by assuming that $S^{(j)}$ is the current value of the conductance and computing the partial derivatives of (28) with respect to d_1 and d_2 after writing $H(s,\omega)$ for SE_d. These give us the two expressions for δE, viz

$$
\begin{aligned}
\delta E_1^{(j)}&(r, 0, \omega) \\
= \ & -\frac{(\delta d_1)2i\omega}{\alpha b} \int_0^c sH(s,\omega)ds \int_0^\infty \lambda e^{-\lambda(d_2 - d_1)} J_1(\lambda r) J_1(\lambda s) \times \\
& \left\{ \frac{\lambda + b/2}{\beta D} + \frac{b}{2D^2} \left[K'_{\nu+1}(\beta)I_{\nu-1}(\alpha) - K_{\nu-1}(\alpha)I'_{\nu+1}(\beta) \right] \right\} d\lambda \\
& -\frac{2(\delta d_1)}{\alpha} \int_0^\infty \frac{\lambda^2 J_1(\lambda r_i)\beta}{D^2} \left\{ \left[K'_{\nu+1}(\beta)I_\nu(\alpha) + I'_{\nu+1}(\beta)K_\nu(\alpha) \right] D \right. \\
& \quad - \left[K_{\nu+1}(\beta)I_\nu(\alpha) + I_{\nu+1}(\beta)K_\nu(\alpha) \right] \times \\
& \left. \quad \left[K'_{\nu+1}(\beta)I_{\nu-1}(\alpha) - I'_{\nu+1}(\beta)K_{\nu-1}(\alpha) \right] \right\} d\lambda,
\end{aligned}
\tag{32}
$$

and

$$
\delta E_2^{(j)}(r, 0, \omega) = \frac{2i\omega(\delta d_2)}{\alpha b} \int_0^c H(s,\omega)s\,ds \int_0^\infty \frac{\lambda^2 J_1(\lambda s) J_1(\lambda r) e^{\lambda(d_1 - d_2)}}{\beta D} d\lambda.
\tag{33}
$$

As before, we can now obtain estimates for the absolute value of the rate of change of the difference norm with respect to the changes in d_1 and d_2.

4   An Application

The results obtained above can be used to estimate the conductance of a conductive body of large lateral extent, located at some depths below the surface of the earth. We will assume that the thickness of the body is small compared to its lateral extent so that it is regarded as a thin circular disk with an unknown conductance. Also, we assume that the electric conductivity of the ground is exponentially decreasing in a manner such that it is negligible after a certain depth, so that it is modelled by an overburden with an exponentially varying conductivity profile. The electromagnetic response on the surface of the earth at a fixed frequency due to a dipole source is calculated if we know the thickness of the overburden, and the radius and conductance for the conductive body.

To generate the data set to be used for the inversion process, we now assume that the disk has a radius of 1000 metres, and is located at a depth of 100 metres beneath an overburden which occupies the first 30 metres from the ground surface. We assume the overburden to have an electric conductivity profile given by $\sigma(z) = \sigma_1 \exp(-0.537z)$, and the disk to have a conductance of 1000 Siemens. In our application, we use the fixed source method, and the data set is generated by measuring the responses at transmitter/receiver separation distances from 20 metres to 210 metres in steps of 10 metres. Random errors up to 3% are superimposed on the scaled electric field from the forward problem to produce the data set $\left\{ \boldsymbol{E}^{(d)} \right\}$ and the result is given in Figures 2–3.
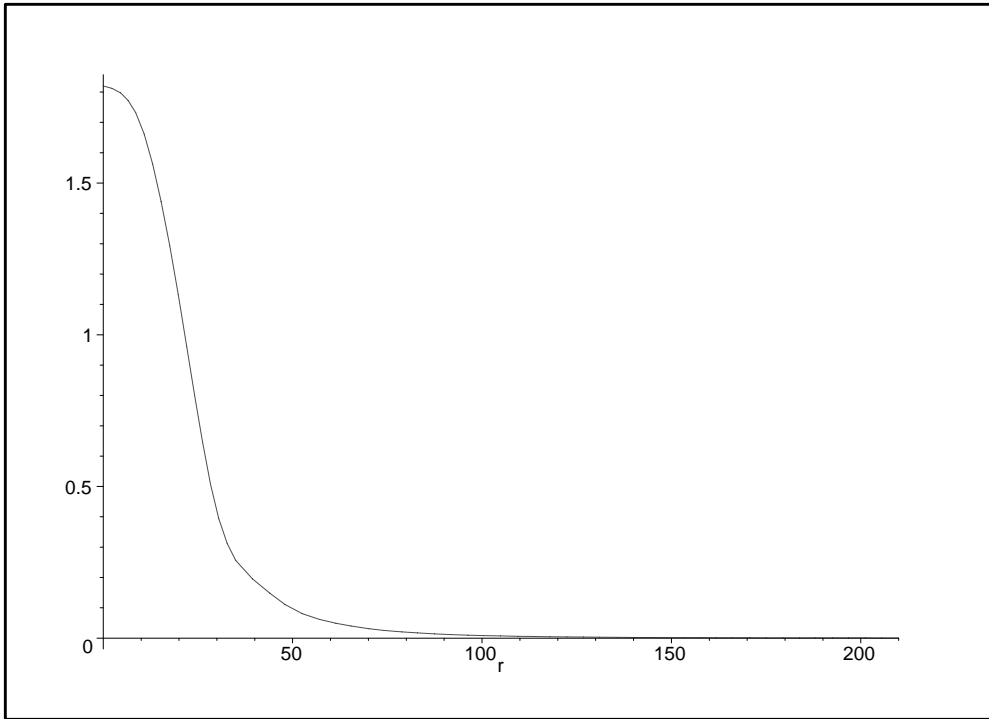
FIGURE 2: Electric field on the ground surface—In phase component.
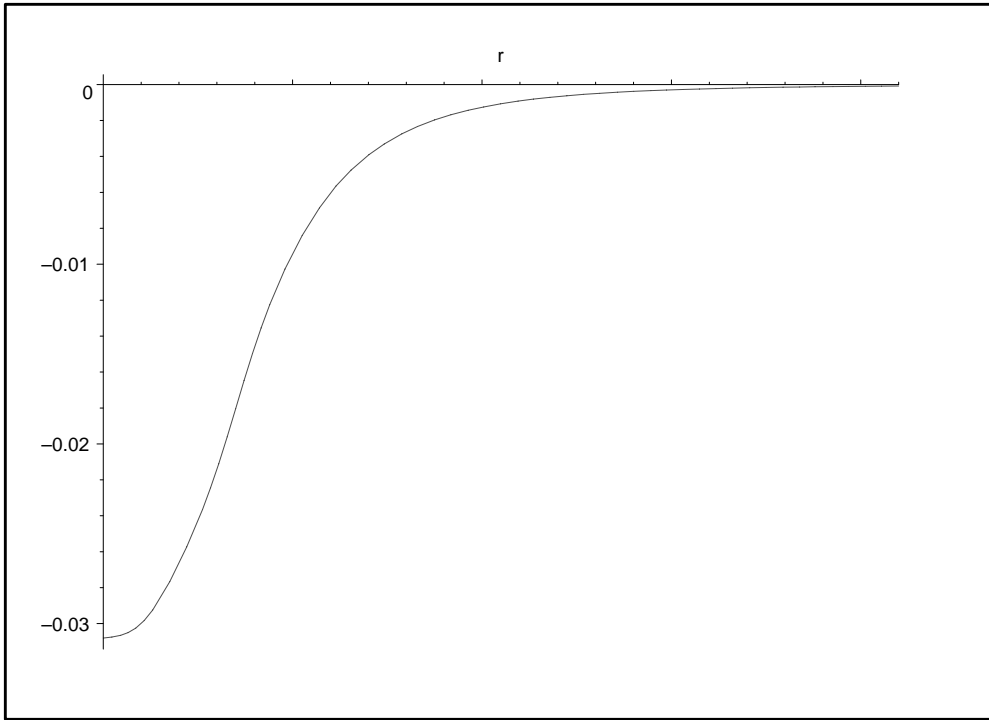
FIGURE 3: Electric field on the ground surface—Quadrature component.

The results of the previous section now allow us to use standard optimisation techniques to estimate the values of d_1, d_2 and S subject to a convergence criterion based on the magnitude of the difference norm ΔE. Starting with guesses for the initial set $\left\{ S^{(0)}, d_1^{(0)}, d_2^{(0)} \right\}$, we estimate the field on the surface of the earth $E^{(0)}(r, 0, \omega)$, and hence obtain the difference norm $\Delta E^{(0)}$. If at the jth step we have $\left\{ S^{(j)}, d_1^{(j)}, d_2^{(j)} \right\}$, we calculate $\Delta E^{(j)}$, and then Equations (31), (32) and (33) are used to determine the next estimates for $\left\{ S^{(j+1)}, d_1^{(j+1)}, d_2^{(j+1)} \right\}$ that are consistent with a decrease in the difference norm. This process is repeated until either the difference norm reaches a prescribed value, or has reached its minimum value. In the results presented here, we have used the method of steepest descent to determine the set of values for the $(j+1)$th step. In terms of computational time, the method is not very economical, however, it serves our purpose in illustrating how the equations we have derived can be used to estimate the unknown parameters of the problem.

Table 1 gives the result of the inversion where four different sets of initial estimates are used for $S^{(0)}$, $d_1^{(0)}$ and $d_2^{(0)}$. At the end of the 5th iteration d_1 is within 1% of its true value, whereas d_2 is less than 5.2% out. The variation of S from its true value is more than 8% out. A comparison of the measured and calculated electric field at this stage does not bring out the differences in accuracy for the estimated parameters. Figure 4 shows the error in the inphase and quadrature components of the estimated electric field at the end of the fifth iteration, expressed as a percentage of the measured field. This error is uniformly small over the range of observations, the largest error be-

i	0	1	2	3	4	5	Optimal
$S^{(i)}$	10000	5000	2500	1250	929.367	1045.54	997.671
$d_1^{(i)}$	10	21.2262	28.5028	31.4246	30.1485	29.7939	30.5838
$d_2^{(i)}$	50	74.9652	88.0724	96.5168	99.4842	101.330	99.0250
$\Delta E^{(i)} \times 10^4$	1.15464	.902420	.695624	.481025	.080557	.416732	
$S^{(i)}$	253.303	379.954	569.932	854.897	961.759	1081.98	1006.62
$d_1^{(i)}$	10	25.3254	29.4879	31.6818	31.3252	29.9951	30.7666
$d_2^{(i)}$	50	73.2578	90.9765	101.571	99.8619	99.4178	100.405
$\Delta E^{(i)} \times 10^4$	.978361	.612957	.391501	.137377	.062623	.102904	
$S^{(i)}$	10000	5000	2500	1250	937.500	1054.69	1004.22
$d_1^{(i)}$	10	24.2669	30.2359	32.3654	30.7354	29.2887	30.6593
$d_2^{(i)}$	150	123.341	116.881	103.230	101.300	98.9379	100.859
$\Delta E^{(i)} \times 10^4$	1.06123	.829868	.588134	.428356	.074753	.302718	
$S^{(i)}$	253.303	379.954	569.932	854.897	961.759	1081.98	1007.28
$d_1^{(i)}$	10	29.6256	34.0411	30.6622	30.2381	29.8612	30.0734
$d_2^{(i)}$	150	128.217	112.070	97.0491	100.315	101.758	100.771
$\Delta E^{(i)} \times 10^4$	1.29693	.979173	.674960	.446488	.074130	.095032	

TABLE 1: Successive iterates using four initial estimates for $\left\{ S^{(0)}, d_1^{(0)}, d_2^{(0)} \right\}$
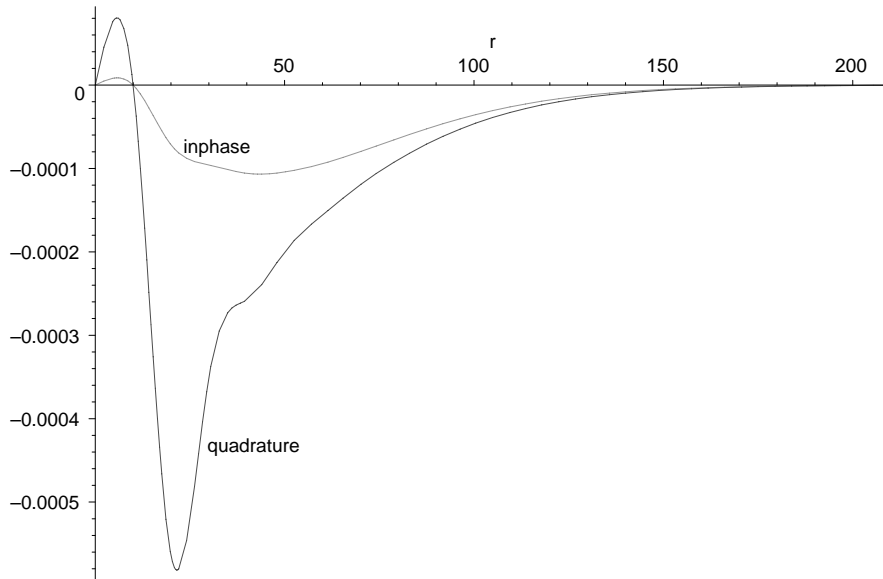
FIGURE 4: Percentage error in the electric field after the fifth iteration.

ing about 0.06% for the quadrature component. Returning to Table 1, we note that, in each case, the difference norm has reached a minimum between the 3rd and 5th iteration. Using the values in the last three iterations, a simple interpolation is made to determine the optimal values for d_1 and d_2, and these values were then used in equations (28) and (29) to calculate the optimal value for S. These optimal values are given in the last column of the table. The optimal value for d_1, in each case, is within 2.6% of its true value, whereas d_2 is less than 1% out. The optimal value for S differs from its true value by less than 0.73%. When the same problem is done with exact data, the corresponding maximum percentage errors in the optimal values of $\{S, d_1, d_2\}$ are found to be 0.9, 1.9 and 0.9 respectively. The relatively large percentage error in the estimates of the thickness (d_1) of the overburden is attributed to the exponential profile used for the conductivity where the rapid exponential decay does not give a sharp interface. Double precision is employed throughout in all the numerical routines used, but where appropriate, only 6 significant figures are kept in the table.

5   Conclusion

The application in the previous section indicates that we have the basis of a simple method for the inverse problem of determining the thickness of the overburden, as well as the depth and conductance of a body that is large in its lateral extent compared to its thickness. The thin disk is located in a resistive

basement under the inhomogeneous conductive overburden. Very accurate estimates for the thickness of the overburden, the depth, and the conductance of the disk is obtained. Although random errors, up to the 3% level have been superimposed on the data set, the optimal values obtained are all well within this level. The method is robust with respect to different starting conditions and it can obviously be adapted to deal with more complicated layered structures.

References

[1] M. Abramowitz and I.A. Stegun (eds.) *Handbook of mathematical functions.* (New York, 1970).

[2] G.E. Backus and J.F. Gilbert, "Numerical applications of a formalism for geophysical inverse problems", *Geophys. J. Roy. Astr. Soc.* **13** (1967) 247–276.

[3] G.E. Backus and J.F. Gilbert, "The resolving power of gross earth data", *Geophys. J. Roy. Astr. Soc.* **16** (1968) 169–205.

[4] A.D. Chave, "Numerical integration of related Hankel transforms by quadrature and continued fraction expansion", *Geophysics* **48** (1983) 1671–1686.

[5] G. Buselli and D.R. Williamson, "Modelling of broadband airborne electromagnetic responses from saline environments", *Geophysics* **61** (1996) 1624–1632.

[6] P.K. Fullagar and D.W. Oldenberg, "Inversion of horizontal loop electromagnetic frequency soundings", *Geophysics* **49** (1984) 150–164.

[7] F.S. Grant and G.F. West, *Interpretation theory in applied geophsysics.* (New York: McGraw-Hill 1965).

[8] H.S. Kim and K. Lee, "Response of a multilayered earth with layers having exponentially varying resistivities", *Geophysics* **61** (1996) 180–191.

[9] T.J. Lee and R. Ignetik, "Transient Electromagnetic Response of a half-space with Exponential Conductivity Profile and its Applications to Salinity Mapping", *Exploration Geophysics* **25** (1994) 39–51.

[10] D.W. Oldenburg, "The interpretation of direct current resistivity measurements", *Geophysics* **43** (1978) 610–625.

[11] R.L. Parker, "The inverse problem of electrical conductivity in the mantle", *Geophysical Journal of the Royal Astronomical Society* **22** (1970) 121–138.

[12] J. Ryu, F. Morrison and S.H. Ward, "Electromagnetic field about a loop source of current", *Geophysics* **35** (1970) 862–896.

[13] P.F. Siew and S. Yooyuanyong, "Inversion by EM sounding for a disk embedded in a conducting half-space", *Tech. Rep.* **20/97** (1997) Curtin University.

[14] G.F. West and R.N. Edwards, "A simple parametric model for the electromagnetic response of an anomalous body in a host medium", *Geophysics* **50** (1985) 2542–2557.